Polysulfone ultrafiltration membrane incorporated with Ag-SiO_2 nanohybrid for effective fouling control

Huiqing Wu, Jing Huang and Yuejun Liu

ABSTRACT

An anti-fouling hybrid membrane was prepared by incorporating Ag-SiO_2 nanohybrid into a polysulfone (PSf) matrix. The addition of Ag-SiO_2 can significantly improve the hydrophilicity, separation property, anti-fouling ability, and especially anti-bacterial activity of hybrid membranes. The optimum performance of the Ag-SiO_2/PSf hybrid membrane is achieved when the concentration of Ag-SiO_2 is as low as 0.45 wt%. Compared with PSf membrane and SiO_2/PSf hybrid membrane, the Ag-SiO_2/PSf hybrid membrane displays the best overall properties. The excellent performance of the Ag-SiO_2/PSf hybrid membrane can be attributed to the well-tailored structure and unique property of Ag-SiO_2 nanohybrid, where nanosized Ag (~5 nm) can densely and uniformly disperse on the surface of silica spheres. The obtained membrane could be a promising material for water treatment.

Key words | anti-fouling, membrane, nanohybrid, polysulfone

Huiqing Wu
Yuejun Liu (corresponding author)
School of Materials Science and Engineering,
Xiamen University of Technology,
600 Ligong Road,
Xiamen,
China
E-mail: *yjliu_2005@126.com*

Jing Huang
State Key Laboratory of Genetic Engineering,
School of Life Sciences, Fudan University,
2205 Songhu Road,
Shanghai,
China

Yuejun Liu
Key Laboratory of New Materials and Technology for Packaging,
Hunan University of Technology,
88 Taishan Road,
Zhuzhou,
China

INTRODUCTION

Membrane separation technology is increasingly applied in water treatment, thanks to the advantages of high efficiency, easy operation, and low cost. During the lengthy separation process, membrane fouling is an inevitable problem causing deterioration in the membrane performance, such as a reduction of flux rate, an elevated operation maintenance cost, and a decrease in the extent of membrane survival (Drews 2010; Zhang *et al.* 2012). Membrane fouling is usually defined as the undesirable deposition of retained particles, colloids, macromolecules, salts, etc. at the membrane surface or at the pore wall inside the pores (Rana & Matsuura 2010). Generally the fouling can be classified into three major categories: organic fouling, inorganic fouling and biofouling (Kappachery *et al.* 2010). Among them, biofouling is regarded as the most complicated one, as a result of the self-replicating nature of biofouling organisms. Even at a low nutrient concentration, a tiny amount of bacteria can grow and multiply rapidly, giving rise to a difficult elimination (Flemming *et al.* 1997). The main approaches to control biofouling include anti-adhesion and anti-microbial methods (Huang *et al.* 2012). Developing a hydrophilic membrane surface is a useful anti-adhesion approach to reduce initial adsorption of bacteria. Regarding an anti-microbial approach, some biocides can be incorporated into the membrane and endow it with the ability to effectively kill bacteria attached on the membrane surface and also prevent their growth.

It has been proved that incorporating inorganic nanoparticles into a membrane matrix is a convenient and useful method for the enhancement of anti-fouling properties (Wang *et al.* 2005; Jeong *et al.* 2007; Lind *et al.* 2009; Qiu *et al.* 2009; Liao *et al.* 2010; Weng *et al.* 2011; Celik *et al.* 2011a, 2011b; Majeed *et al.* 2012). Some hydrophilic inorganic nanoparticles, such as carbon nanotube, graphene oxide, and zeolite, help the hydrophilicity and, correspondingly, anti-adhesion ability of membranes (Wang *et al.* 2005; Choi *et al.* 2006; Jeong *et al.* 2007; Lee *et al.* 2008; Lind *et al.* 2009; Qiu *et al.* 2009; Liao *et al.* 2010; Sun *et al.* 2010; Wu *et al.* 2010, 2012, 2013a, 2013b; Celik *et al.* 2011a, 2011b; Majeed

doi: 10.2166/wh.2017.234

et al. 2012); moreover, some specific nanoparticles that exhibit inhibitory and bactericidal effects, directly contribute to the anti-microbial ability of membranes. Especially, silver has attracted much interest due to its high toxicity toward many types of bacteria and low toxicity for humans and animals (Tenover 2006). Various membranes such as polysulfone (PSf), polyethersulfone, polyamide, polyacrylonitrile, chitosan, and cellulose acetate decorated with silver have been fabricated for performance improvement (Chou *et al.* 2005; Taurozzi *et al.* 2008; Zodrow *et al.* 2009; Basri *et al.* 2010, 2012; Cao *et al.* 2010; Zhang *et al.* 2012, 2013; Huang *et al.* 2012, 2014; Yin *et al.* 2013; Liu *et al.* 2013). Furthermore, Mollahosseini *et al.* (2012) found silver nanoparticle size had a significant effect on the anti-bacteriality of membrane and the hybrid membrane with smaller silver nanoparticles had better properties. Silver nanoparticles of less than 10 nm were more effective for anti-biofouling (Gunawan *et al.* 2011). However, silver nanoparticles commonly produced by chemical reduction usually encounter a serious problem in that nanoparticles are less stable and tend to aggregate when the average particle size is less than 40 nm. This definitely reduces improvement in membrane performance (Mafune *et al.* 2000; Jiang *et al.* 2006).

To overcome the problems mentioned above and thus achieve better membrane performance, Ag-SiO_2 nanohybrid was prepared and then used to functionalize polymer membrane. Yu *et al.* (2013) observed maximal water flux (~150% higher than that of pure PES membrane) and a good antibacterial effect of Ag-SiO_2/polyethersulfone (PES) hybrid membrane prepared at the nanohybrid concentration of 2.68% in the casting solution. Huang *et al.* (2014) focused on the anti-bacterial and anti-formation properties of Ag-SiO_2/PES hybrid membrane, and found the membrane with 2% Ag-SiO_2 nanohybrid displayed the best overall performance.

Herein, the microstructure of nanohybrid has a significant effect on the membrane performance; the concentration of nanohybrid is also crucial because a high addition of nanohybrid could easily have some negative effect, such as particle aggregation, membrane structure change, and deterioration of membrane properties. Thus, in this study, the structure of Ag-SiO_2 was precisely tailored to take full advantage of this nanohybrid and exploit a systematic research. It should be emphasized that Ag with a particle size of approximately 5 nm can disperse densely and uniformly on the surface of a silica sphere (~150 nm). The unique structure of Ag-SiO_2 nanohybrid can not only effectively reduce the aggregation of nanoscale-sized Ag, but also result in an extremely high hydrophilicity of hybrid particles. PSf is used as the membrane matrix in this study, because it has been widely used as an ultrafiltration membrane material in many industrial fields due to its low cost, superior film-forming ability, good mechanical and anti-compaction properties, and strong chemical and thermal stabilities. Subsequently, low concentrations of Ag-SiO_2 nanohybrid (0.15 wt% ~ 0.75 wt%) were introduced into the PSf matrix to study the improvement of hybrid membrane performance. Transmission electron microscopy (TEM) with energy-dispersive X-ray analysis (EDX), X-ray diffraction (XRD) and UV-vis were employed for the characterization of Ag-SiO_2. Then, separation properties including pure water flux and rejection, anti-fouling and antibacterial behaviors were investigated to gain a deep insight into the influence of Ag-SiO_2 morphology and loading on the membrane performance. Furthermore, Ag releasing behavior was also tested for the stability of silver in a hybrid membrane.

EXPERIMENTAL

Materials

Commercial PSf, Udel P3500, was purchased from Boji Co., Ltd. Polyvinylpyrrolidone (PVP), tetraethyl orthosilicate (TEOS), aqueous ammonia (25% w/w), and N-methyl-2-pyrrolidone (NMP) were bought from Aladdin Co., Ltd. C_2H_5OH, NaOH, silver nitrate ($AgNO_3$), and bovine serum albumin (BSA) were purchased from Sinopharm Chemical Reagent Co., Ltd and used as received. Egg albumin with an average molecular weight of 45,000 g/mol was used as a probe molecule for rejection tests and supplied by Sinopharm Chemical Reagent Co., Ltd.

Preparation of inorganic particles

Synthesis of silica particles (SiO_2)

To a flask, 50 mL of EtOH, 1 mL of H_2O, and 3 mL of aqueous ammonia were added. A volume of 1.5 mL of TEOS

was rapidly added to the flask and magnetically stirred (300 rpm) for 3 h at 40 °C. The SiO_2 was harvested by centrifugation, washed with copious ethanol, and then dispersed in ethanol at 2–3% silica concentration for subsequent use.

Synthesis of Ag-SiO_2 nanohybrid

Ag-SiO_2 nanohybrid was synthesized as follows (Deng *et al.* 2007). A 10 mL quantity of freshly prepared $[Ag(NH_3)_2]^+$ ion solution was quickly added to 10 g of SiO_2/EtOH solution under magnetic stirring at room temperature for 1.5 h. Then, 50 mL of ethanol containing PVP (0.5 mmol/L) was added for stabilization and reduction, and the mixture was stirred at 70 °C for 7 h. The product was collected by centrifugation and finally dried.

Membrane preparation

The PSf-based hybrid membranes were prepared by incorporating Ag-SiO_2 nanohybrid via phase inversion method. The detailed procedure of membrane preparation can be obtained from our recent work (Wu *et al.* 2012). First, an approximately 15 wt% PSf homogeneous solution with a given amount of Ag-SiO_2 nanohybrid (the particle concentrations in the casting solution varied from 0.15 wt% to 0.75 wt%) was prepared. Next, the mixture solution was cast onto a glass plate and immersed in deionized (DI) water at a temperature of 30 °C for at least 24 h. The thickness of the membrane was approximately 100 μm.

Characterization

Membrane characterization

Particles were observed by transmission electron microscope (Hitachi H-600). XRD patterns were acquired by a D8 ADVANCE and DAVINCI.DESIGN (Bruker) X'pert diffractometer with Cu Kα radiation. The size distribution of the particles was measured by dynamic light scattering (DLS) using a Zetasizer Nano measurement. UV-visible absorption spectra were recorded using a UV-visible spectrophotometer (Hitachi U-2910).

The surfaces and cross-sections of membrane were observed using a scanning electron microscope (SEM; TESCAN 5136MM) and high-resolution FE-SEM S-4800 equipped with energy-dispersive spectrometer (TEM-QUANTAX 400, Bruker). Cross-sectional membrane samples were obtained by previous freeze fracturing after immersion in liquid nitrogen.

The static contact angle of water on the surface of a polymer membrane was measured by using OCA15 (Dataphysics Co., Germany) for determination of the hydrophilicity. The average value of the contact angle on each polymer membrane was calculated using at least five different locations on each membrane.

Flux and separation experiments

The measurements of pure water flux and protein rejection were performed using a cross-flow membrane module as described in our previous paper (Wu *et al.* 2012). The operation pressure was 0.2 MPa. Before the measurements, all the membranes were pretreated for about 10 min and then the pure water flux and rejection were measured. The water flux (F) was calculated using Equation (1):

$$F = \frac{V}{At} \tag{1}$$

where V is the total volume of permeated pure water (L), A is the effective membrane area (m^2), and t is the operation time (h). The rejection (R) was measured with 0.5 g/L egg albumin solution, and calculated using Equation (2):

$$R = \frac{1 - C_p}{C_f} \tag{2}$$

where C_p and C_f are the concentrations of the permeation and feed solutions, respectively. The concentrations of the feed and permeate solutions were determined by an ultraviolet–visible spectrophotometer (Hitachi U-2910) at 205 nm. The results shown were calculated from at least three membranes.

Anti-organic fouling and anti-biofouling test

Measurements for organic fouling resistance of membrane were performed as follows (Wu *et al.* 2012). First, distilled water passed through the membrane for 60 min at an

operation pressure of 0.2 MPa, and the water flux (J_1) reached a stable stage. Second, feed solutions (1.0 mg/mL BSA solution, pH was kept at 7.0 with 0.1 M phosphate buffer solution) were filtrated for 60 min at 0.2 MPa, and the flux for protein solution (J_p) was determined. After ultrafiltration of BSA solution, the membranes were simply washed by immersing them into DI water for 15 min under stirring, then the pure water flux of cleaned membranes (J_2) was measured again. Several ratios, including flux recovery ratio (*FRR*), total fouling ratio (R_t), irreversible fouling ratio (R_{ir}), and reversible fouling ratio (R_r), were defined to describe the organic fouling resistance of membranes to analyze the fouling process, and calculated as follows: $FRR = J_2/J_1$, $R_t = 1 - J_p/J_1$, $R_{ir} = (J_1 - J_2)/J_1$, $R_r = (J_2 - J_p)/J_1$, $R_t = R_{ir} + R_r$, respectively.

The anti-biofouling ability of prepared membranes was evaluated by inhibition zone method against *Escherichia coli*. Before the test, *E. coli* strain was first cultured in a flask, and then the prepared *E. coli* solution was pipetted onto a plate and spread throughout the surface. A circular disk of each membrane (d = 19 mm) was placed on the bacterial surface to incubate for 24 h at 37 °C. After that, the inhibition rings that formed around the membranes could serve as an indicator for antibacterial performance, and were visually observed with a digital camera.

Silver releasing test

The releasing behavior of silver nanoparticles from the Ag-SiO_2/PSf hybrid membrane was investigated. Hybrid membrane with 0.45 wt% of Ag-SiO_2 was chosen for the test. The membrane was cut into 1 cm^2 pieces, and the samples were immersed in 10 mL deionized water at room temperature. The water was replaced every 24 h and collected. Finally, all the samples were acidified by 1% HNO_3 and analyzed by atomic adsorption spectrometer (Hitachi Z-5000).

RESULTS AND DISCUSSION

Characterization of Ag-SiO_2 nanohybrid

As shown in Figure 1(a) and 1(b), the silica substrates are uniform spheres with a mean diameter of approximately 150 nm. The result of DLS measurement suggests SiO_2 particles have a mean diameter of 204.4 nm with a narrow size distribution (PDI =0.068), slightly larger than observed from TEM due to the hydrate layer in aqueous environment. A dense and uniform coverage of silver nanoparticles formed on the surface of silica spheres. As seen clearly from the TEM image with high magnification (Figure 1(c)), the size of silver nanoparticles is only about 5 nm, and the nanosized Ag disperse well on the silica surface without obvious aggregation. The fine structure of Ag-SiO_2 nanohybrid is expected to benefit the high hydrophilicity and anti-bacteriality of particles and, correspondingly, those of hybrid membrane. Furthermore, as shown in the EDX spectrum of Ag-SiO_2 (Figure 1(d)), the weight percent of Ag in the Ag-SiO_2 is estimated to be as high as ~16%, proving the high density of Ag nanoparticles that grow on SiO_2 surface.

The XRD spectrum of Ag-SiO_2 is depicted in Figure 2(a). The peaks at 2θ of 37.9 °, 44.1 °, 64.3 °, 77.2 °, and 81.4 °, are respectively attributed to the reflections of (111), (200), (220), (311), and (222) crystalline planes of the *fcc* structure of Ag, indicating the crystallinity of Ag nanoparticles. The results of UV-visible scan measurement are illustrated in Figure 2(b). Bare SiO_2 does not present any absorption, while Ag-SiO_2 displays an obvious absorption peak at around 420 nm, as a result of Mie Plasmon resonance excitation from the silver nanoparticles (Deng *et al.* 2007). In addition, it is also observed that the supernatant of Ag-SiO_2 nanohybrid after centrifugation presents no Plasmon resonance peak at 420 nm, demonstrating that most of the Ag nanoparticles are formed on the silica spheres rather than in the suspension.

Effect of Ag-SiO_2 loading on the membrane properties

To study the influence of Ag-SiO_2 nanohybrid loading on the membrane performance and morphology, the casting solution containing Ag-SiO_2 content from 0.15 wt% to 0.75 wt% was used for membrane preparation. Figure 3 demonstrates a plot of pure water flux and rejection to egg albumin vs. Ag-SiO_2 content. The pure water flux of the membrane significantly increases along with the number of Ag-SiO_2 particles in the membrane. When 0.45 wt% of Ag-SiO_2 is added, the water flux reaches a value which is about twice that of the PSf membrane, and it keeps

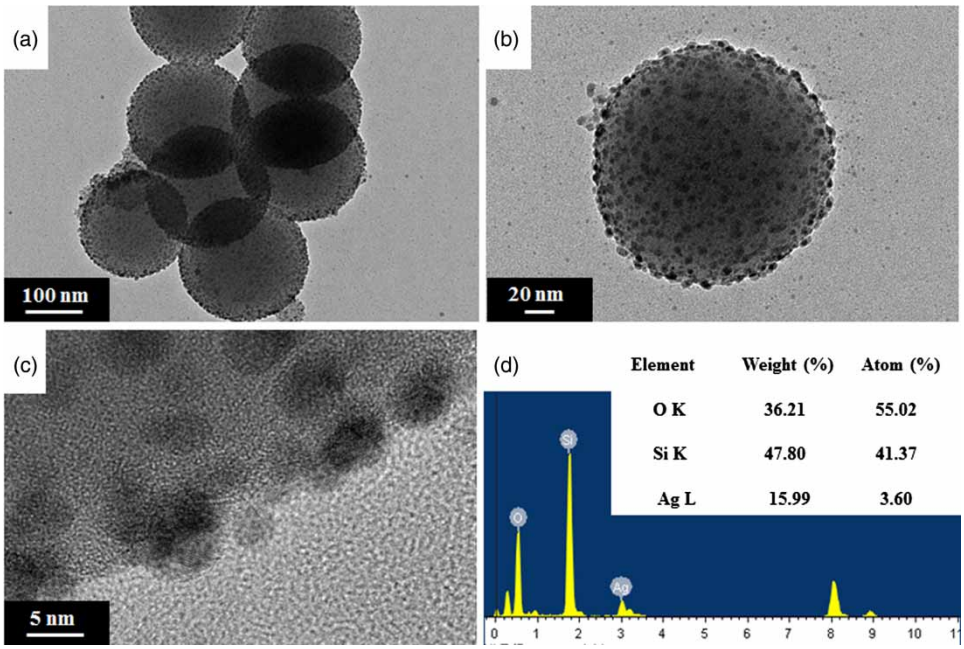

Figure 1 | (a)–(c) TEM images of Ag-SiO_2 and (d) EDX spectrum of Ag-SiO_2.

increasing with higher content of Ag-SiO_2, illustrating a good dispersion of Ag-SiO_2 hybrid in the membrane matrix. The improvement of water flux can be mainly attributed to the high hydrophilicity of Ag-SiO_2 nanohybrid. First, Ag-SiO_2 with high hydrophilic surface promotes the hydrophilicity of the membrane, promoting the interaction between membrane and water molecules and thus contributing to the water transport rate. As shown in Figure 4, the water contact angle of the hybrid membrane decreased with the Ag-SiO_2 loading, suggesting an increase in the hydrophilicity of the hybrid membrane and also serving as a proof for the analysis above. Second, the enhanced hydrophilicity of casting solution produced by the addition of hydrophilic Ag-SiO_2 nanohybrid accelerates the exchange rate between solvent and nonsolvent during phase inversion, leading to the formation of the membrane structure with a larger pore size and, correspondingly, the improvement of water flux (Choi *et al.* 2006; Stankovich *et al.* 2007; Qiu *et al.* 2009). From the SEM images of a cross-section of the hybrid membrane in Figure 5, it can be observed that the membrane incorporated with more Ag-SiO_2 possesses a pore structure with slightly larger size.

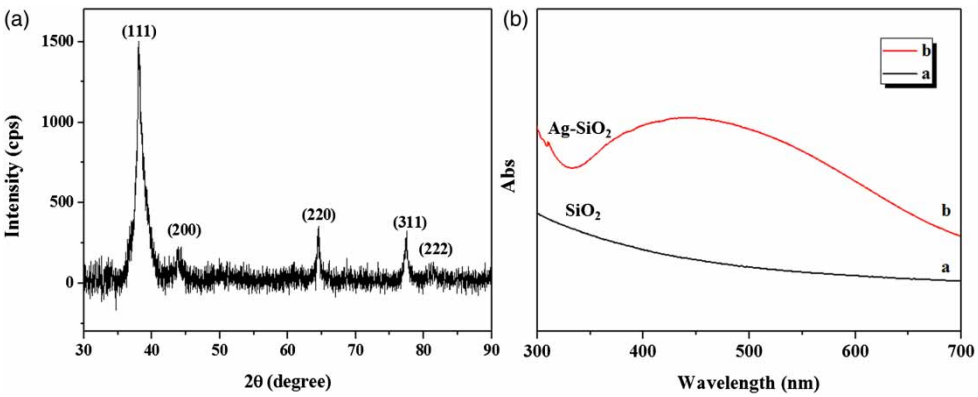

Figure 2 | (a) XRD pattern of Ag-SiO_2; (b) UV-visible absorption spectra of bare silica particles and Ag-SiO_2 nanohybrid.

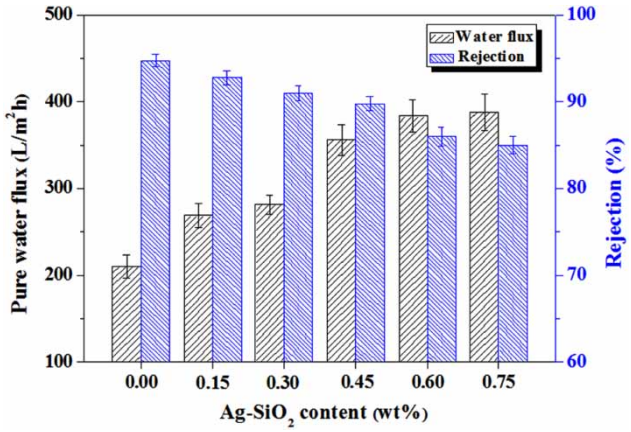

Figure 3 | Effect of Ag-SiO_2 content in the casting solution on the pure water flux and rejection to egg albumin of Ag-SiO_2/PSf hybrid membranes at 0.2 MPa operation pressure.

Accordingly, the egg albumin rejection decreases with increasing amounts of Ag-SiO_2. From the results, it can be concluded that the hybrid membrane with 0.45 wt% of Ag-SiO_2 exhibits the best overall property including water flux and egg albumin rejection. Compared with the work reported (Yu *et al.* 2013; Huang *et al.* 2014), a significant enhanced separation property of hybrid membrane can be achieved at such a low content of Ag-SiO_2, probably due to the well-tailored microstructure of Ag-SiO_2 nanohybrids.

The surface morphologies of membranes with different loading of Ag-SiO_2 were also observed, as shown in Figure 6. The surface of the hybrid membrane becomes rougher as the content of Ag-SiO_2 in the membrane increases, as a result of accelerated exchange rate of solvent and nonsolvent of hydrophilic casting solution during the phase inversion. Moreover, some inorganic particles are found to be incorporated on the membrane surface because hydrophilic inorganic particles, such as Ag-SiO_2, tend to move toward the membrane surface during the phase inversion process. The roughness of the membrane surfaces can be quantified from the atomic force microscopy (AFM) results, as presented in Figure 7. The root mean square roughness of the membranes increases along with the content of Ag-SiO_2 in the matrix, which is consistent with the morphologies observed by SEM images.

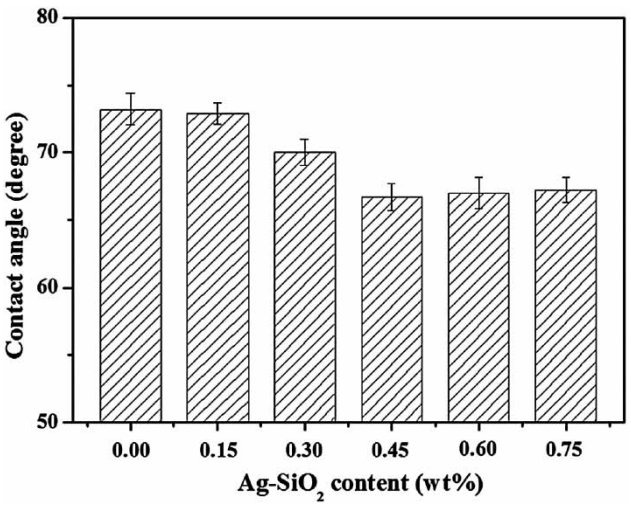

Figure 4 | Contact angles of Ag-SiO_2/PSf hybrid membranes against water as a function of Ag-SiO_2 content in the casting solution.

The anti-biofouling ability of hybrid membranes with different Ag-SiO_2 loading was evaluated by inhibition zone method against *E. coli*. In Figure 8, pure PSf membrane and SiO_2/PSf hybrid membrane show no obvious inhibition rings while all of the hybrid membranes incorporated with Ag-SiO_2 present the inhibition effect around them. With the increase of Ag-SiO_2 content, the inhibition zone became clearer and wider, illustrating the contribution of Ag-SiO_2 to the anti-bacterial activity of hybrid membranes. It is expected to be attributable to two factors, that is, on the one hand, the adhesion of bacteria to Ag-SiO_2/PSf hybrid membrane surface is more difficult with an enhanced hydrophilicity; on the other hand, the adhered bacteria would be killed or their growth suppressed by Ag on the membrane surface.

Characterization of Ag-SiO_2/PSf hybrid membrane

To gain a deep insight into the properties of the Ag-SiO_2/PSf hybrid membrane, hybrid membranes with 0.45 wt% of Ag-SiO_2 were further characterized by EDX, silver releasing measurement, anti-organic fouling, and anti-biofouling test. First, the EDX spectrum was employed to characterize Ag-SiO_2 nanohybrid's dispersion in the PSf membrane matrix by displaying elements in the membrane matrix. Figure 9(a)–9(c) show the SEM image of the surface, Si-mapping, and Ag-mapping image of the EDX of the corresponding membrane, respectively. The EDX mapping images illustrate that Si and Ag are dispersed uniformly in the whole PSf matrix without obvious aggregation. Therefore, it can be deduced that the Ag-SiO_2 nanohybrid has a good distribution in the membrane matrix. The cross-section of

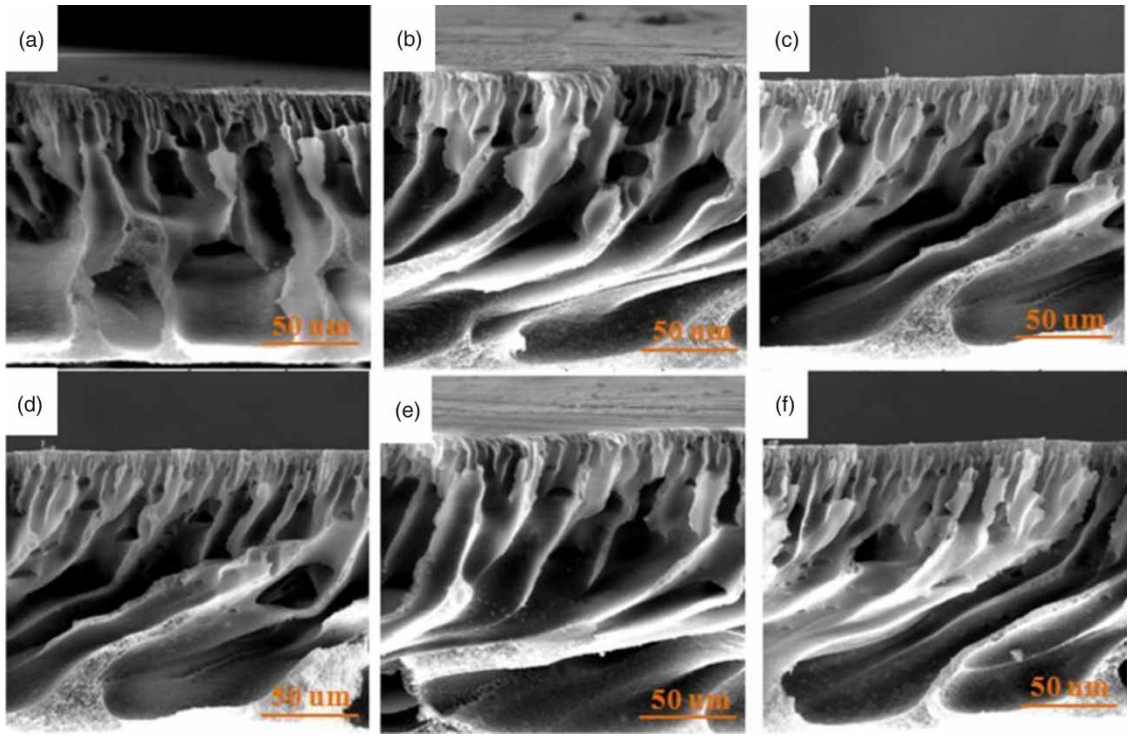

Figure 5 | SEM images of the cross-sections of Ag-SiO_2/PSf membranes with different contents of Ag-SiO_2: (a) 0 wt%; (b) 0.15 wt%; (c) 0.3 wt%; (d) 0.45 wt%; (e) 0.60 wt%; (f) 0.75 wt%.

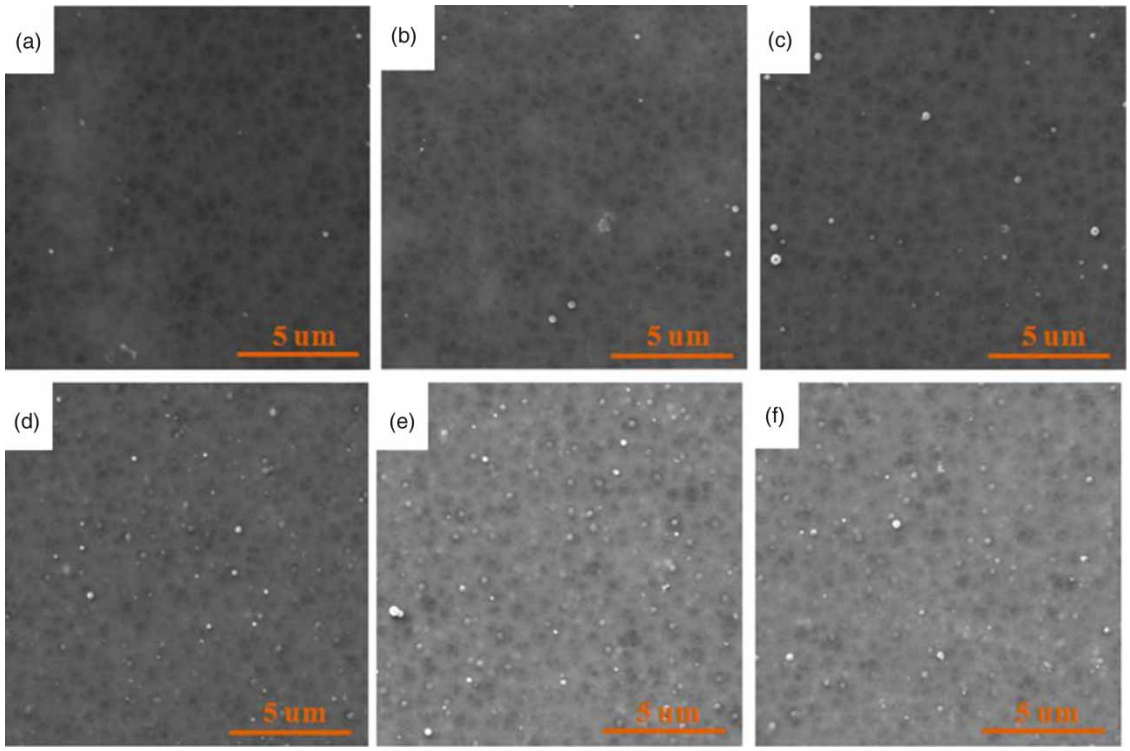

Figure 6 | SEM images of the surfaces of Ag-SiO_2/PSf hybrid membranes with different contents of Ag-SiO_2: (a) 0 wt%; (b) 0.15 wt%; (c) 0.3 wt%; (d) 0.45 wt%; (e) 0.60 wt%; (f) 0.75 wt%.

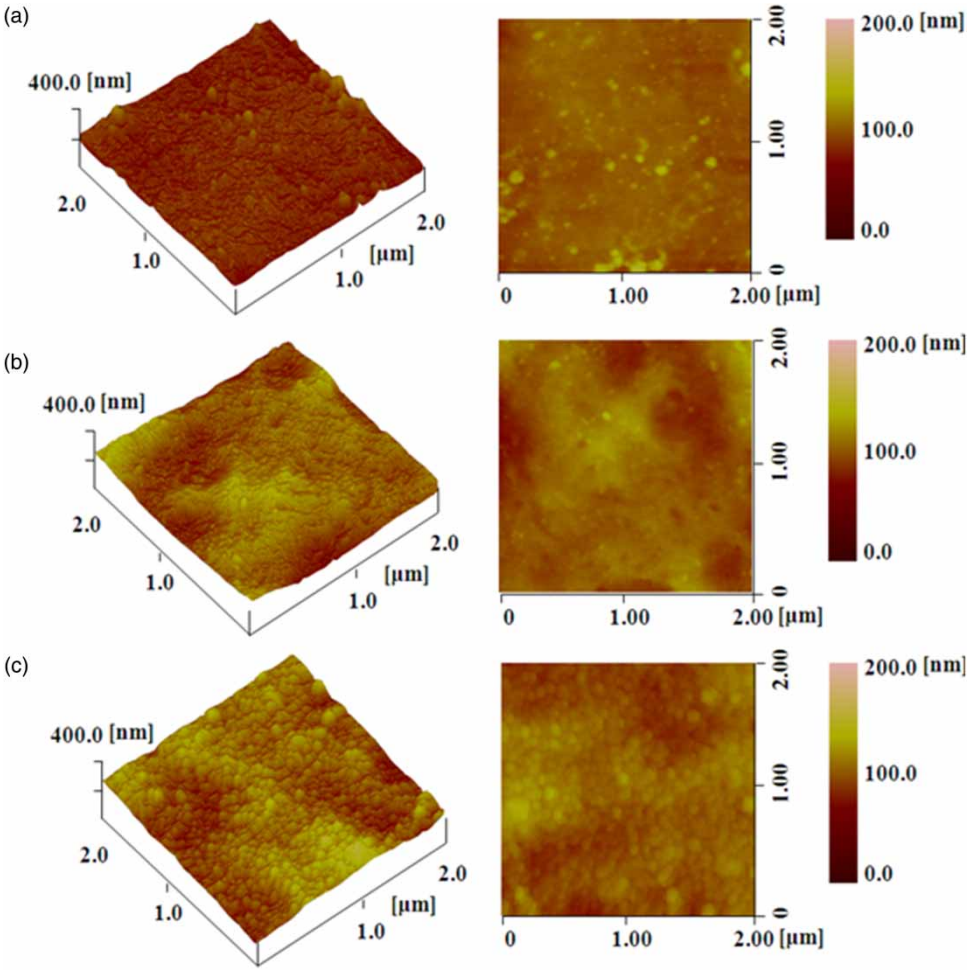

Figure 7 | AFM images of the surfaces of the Ag-SiO_2/PSf hybrid membranes with different contents of Ag-SiO_2: (a) 0 wt%; (b) 0.45 wt%; (c) 0.75 wt%.

hybrid membrane (Figure 9(d)) was also observed by SEM to investigate the dispersion of Ag-SiO_2 within the membrane matrix. Ag-SiO_2 nanohybrids (as the arrows indicate) are well dispersed in the membrane matrix without apparent segregation or agglomeration. In addition, it is found that more Ag-SiO_2 particles are located on the top layer of membrane, probably leading to more direct contact with pollutant and, correspondingly, better anti-fouling performance.

The releasing behavior of Ag from the Ag-SiO_2/PSf hybrid membrane is depicted in Figure 10. According to reports of the World Health Organization (WHO) in 2004, amounts of silver less than 0.1 mg/L are considered totally safe and can be tolerated by the human body. As shown in Figure 10, after 4 day's pretreatment by water, the silver release from hybrid membrane is in the safe range. It is calculated that most silver (~94%) remains in the membrane matrix after 4 day's pretreatment reaching a steady state of low release rate. Furthermore, considering the low release rate of less than 0.1 mg/(L·day) at the steady state, properties of the membranes such as separation performance and antibacterial ability are expected to be effective for months.

For further investigation of the advantages of incorporation of Ag-SiO_2 on membrane performance, pristine PSf membrane and SiO_2/PSf hybrid membrane were prepared and compared with Ag-SiO_2/PSf hybrid membrane in terms of water flux, rejection to egg albumin, contact angle, and anti-fouling ability, respectively. Herein, the contents of inorganic particles in the casting solution are both 0.45 wt%.

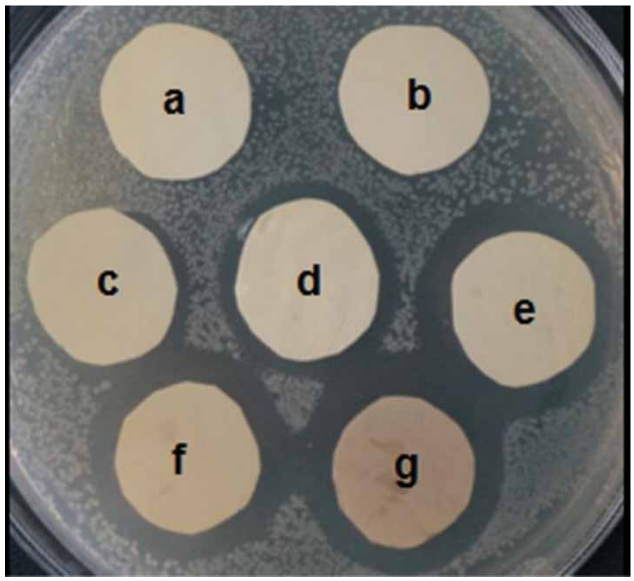

Figure 8 | The anti-bacterial results for *E. coli* on the different membranes: (a) pure PSf membrane; (b) SiO_2/PSf hybrid membrane with 0.45 wt% SiO_2; Ag-SiO_2/PSf hybrid with different contents of Ag-SiO_2: (c) 0.15 wt%, (d) 0.3 wt%, (e) 0.45 wt%, (f) 0.6 wt%, (g) 0.75 wt%.

The performance of membranes with different components is summarized in Figure 11. Compared with pristine PSf membrane, both hybrid membranes display an increased pure water flux with the rejection maintaining at a relatively high level (>90%). Especially, Ag-SiO_2/PSf hybrid membrane has a significant advantage over the water flux rate, as a result of the synergistic effect of nano-sized Ag and SiO_2 from nanohybrid contributing to the extremely high hydrophilicity of Ag-SiO_2. The results of contact angle measurement (Figure 12) are consistent with the analysis above.

Experiments to measure the organic fouling resistance of membranes were performed, and herein BSA is used as organic pollutant. Here, the values of anti-fouling properties are calculated using the parameters of the first circle of membrane fouling and washing. As shown in Figure 13(b) and 13(c), the *FRR* value of Ag-SiO_2/PSf hybrid membrane is the highest, and that of PSf membrane is the lowest. Furthermore, the R_{ir} value of Ag-SiO_2/PSf hybrid membrane is

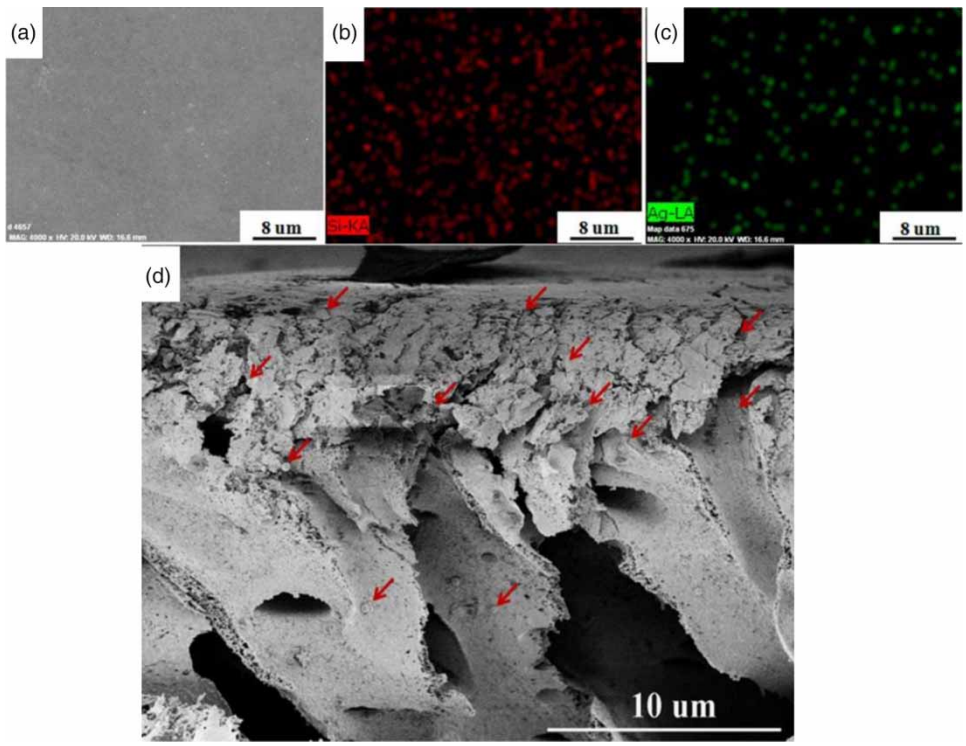

Figure 9 | (a) SEM image of the surface of Ag-SiO_2/PSf hybrid membrane with 0.45 wt% of Ag-SiO_2 nanohybrid; (b) Si-mapped distribution of the corresponding membrane; (c) Ag-mapped distribution of the corresponding membrane; (d) SEM image of the cross-section of the hybrid membrane.

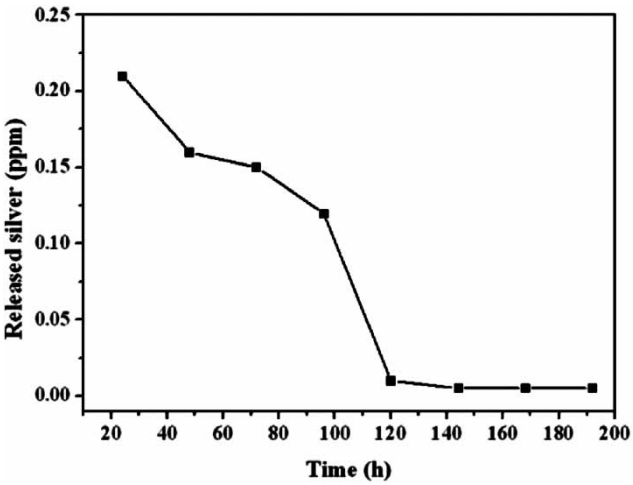

Figure 10 | The silver release measurement of Ag-SiO_2/PSf hybrid membrane.

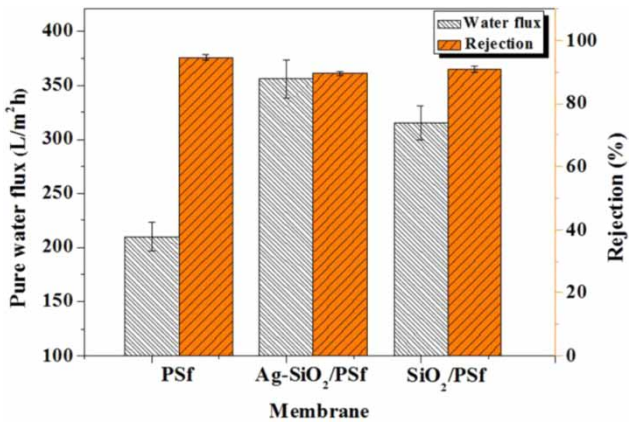

Figure 11 | Performance of membranes with different components.

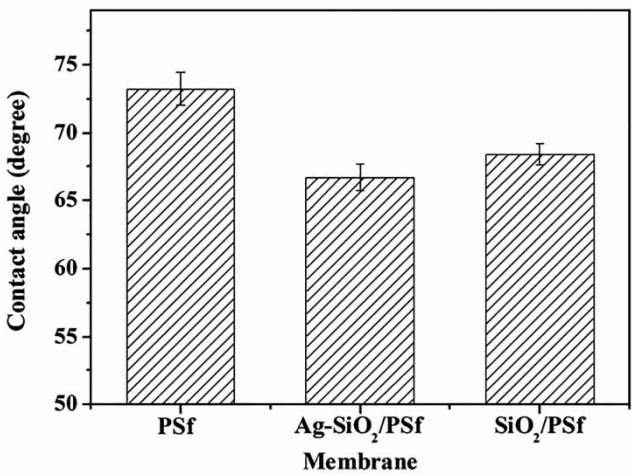

Figure 12 | Contact angles of membranes with different components.

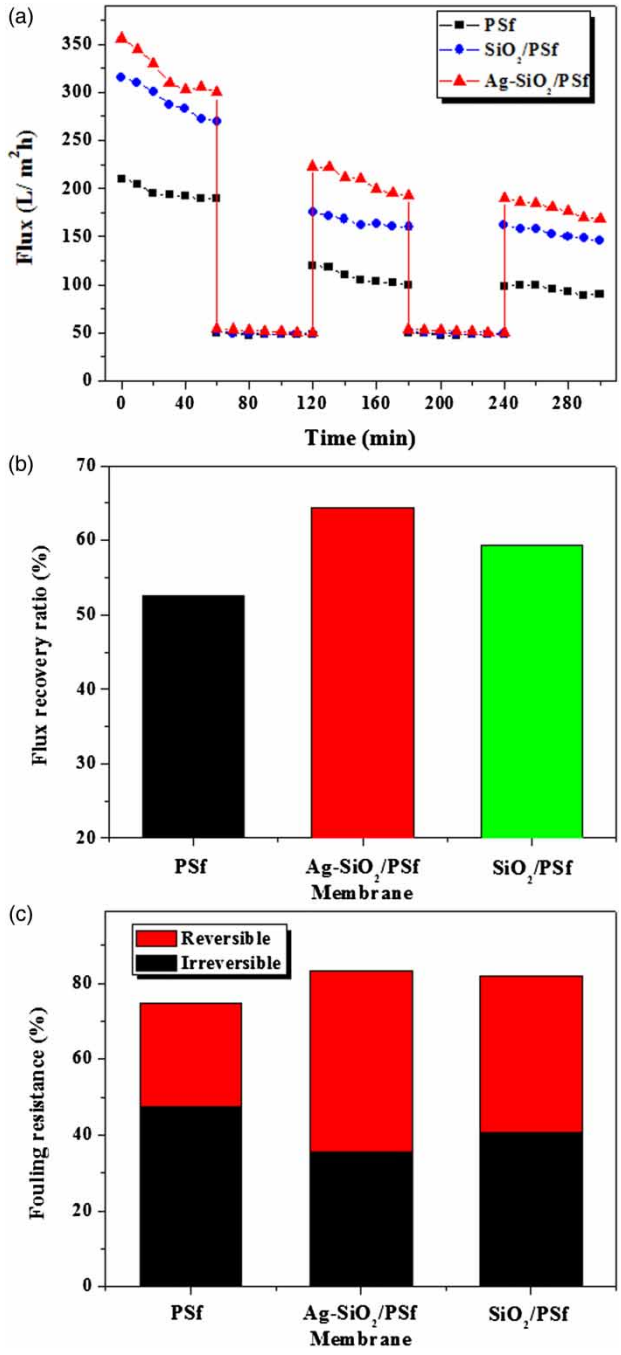

Figure 13 | (a) Time-dependent fluxes of membranes with different components during anti-fouling experiment with BSA filtration (1 mg/mL, pH =7) at 0.2 MPa; (b) *FRR* of the membranes; (c) fouling resistance of the membranes.

sharply reduced to nearly one-third in the total fouling by simply cleaning, while that of PSf membrane is as high as 63%. This is because the loading of hydrophilic SiO_2 and Ag-SiO_2 particles endow strong hydrophilicity to the PSf

membranes, minimizing the hydrophobic interaction between the membrane and proteins, and also promoting the hydrogen bonding between the hydroxyl groups of SiO_2 and water molecules. The higher the hydrophilicity, the better the anti-fouling performance. Consequently, it can be clarified that the addition of high hydrophilic Ag-SiO_2 nanohybrid has the greatest improvement on the ability of organic fouling resistance of membranes.

CONCLUSIONS

Ag-SiO_2 nanohybrid was prepared, and then employed to prepare anti-fouling PSf-based hybrid membrane. In the structure of Ag-SiO_2, nanosized Ag (~5 nm) densely and uniformly disperse on the surface of silica spheres, and this fine microstructure contributes to the high hydrophilicity and anti-bacterial ability of nanohybrid. The obtained Ag-SiO_2 could significantly improve the hydrophilicity, separation property, organic fouling resistance ability, and especially anti-bacterial activity of Ag-SiO_2/PSf hybrid membrane. The results indicate that the hybrid membrane with a low content of Ag-SiO_2 (0.45 wt%) displays the best overall properties, which have obvious advantages over PSf membrane and SiO_2/PSf hybrid membrane.

ACKNOWLEDGEMENTS

The present study was supported by the National Natural Science Foundation of China (No. 11372108), the Natural Science Foundation of Hunan Province, China (No. 14JJ5021), Open Fund Project Innovation Platform of University in Hunan Province, China (No. 20161006), Open Fund Project Innovation Platform of State Key Laboratory of Molecular Engineering of Polymers (Fudan University) (K2017-29) and High-level talents support plan of Xiamen University of Technology (No. YKJ16001R).

REFERENCES

Basri, H., Ismail, A. F., Aziz, M., Nagai, K., Matsuura, T., Abdullah, M. S. & Ng, B. C. 2010 Silver-filled polyethersulfone membranes for antibacterial applications – effect of PVP and TAP addition on silver dispersion. *Desalination* **261**, 264–271.

Basri, H., Ismail, A. F. & Aziz, M. 2012 Microstructure and anti-adhesion properties of PES/TAP/Ag hybrid ultrafiltration membrane. *Desalination* **287**, 71–77.

Cao, X., Tang, M., Liu, F., Nie, Y. & Zhao, C. 2010 Immobilization of silver nanoparticles onto sulfonated polyethersulfone membranes as antibacterial materials. *Colloids Surfaces B* **81**, 555–562.

Celik, E., Liu, L. & Choi, H. 2011a Protein fouling behavior of carbon nanotube/polyethersulfone composite membranes during water filtration. *Water Res.* **45**, 5287–5294.

Celik, E., Park, H., Choi, H. & Choi, H. 2011b Carbon nanotube blended polyethersulfone membranes for fouling control in water treatment. *Water Res.* **45**, 274–282.

Choi, J. H., Jegal, J. & Kim, W. N. 2006 Fabrication and characterization of multi-walled carbon nanotubes/polymer blend membranes. *J. Membr. Sci.* **284**, 406–415.

Chou, W. L., Yu, D. G. & Yang, M. C. 2005 The preparation and characterization of silver-loading cellulose acetate hollow fiber membrane for water treatment. *Polym. Adv. Technol.* **16**, 600–607.

Deng, Z. W., Chen, M. & Wu, L. M. 2007 Novel method to fabricate SiO_2/Ag composite spheres and their catalytic, surface-enhanced Raman scattering properties. *J. Phys. Chem. C.* **111**, 11692–11698.

Drews, A. 2010 Membrane fouling in membrane bioreactors – characterisation, contradictions, cause and cures. *J. Membr. Sci.* **363**, 1–28.

Flemming, H. C., Schaule, G., Griebe, T., Schmitt, J. & Tamachkiarowa, A. 1997 Biofouling – the Achilles heel of membrane processes. *Desalination* **113**, 215–225.

Gunawan, P., Guan, C., Song, X. H., Zhang, Q. Y., Leong, S. S. J., Tang, C. Y., Chen, Y., Chan-Park, M. B., Chang, M. W., Wang, K. A. & Xu, R. 2011 Hollow fiber membrane decorated with Ag/MWNTs: toward effective water disinfection and biofouling control. *ACS Nano* **5**, 10033–10040.

Huang, J., Arthanareeswaran, G. & Zhang, K. S. 2012 Effect of silver loaded sodium zirconium phosphate (nanoAgZ) nanoparticles incorporation on PES membrane performance. *Desalination* **285**, 100–107.

Huang, J., Wang, H. T. & Zhang, K. S. 2014 Modification of PES membrane with Ag-SiO_2: reduction of biofouling and improvement of filtration performance. *Desalination* **336**, 8–17.

Jeong, B. H., Hoek, E. M. V., Yan, Y. S., Subramani, A., Huang, X. F., Hurwitz, G., Ghosh, A. K. & Jawor, A. 2007 Interfacial polymerization of thin film nanocomposites: a new concept for reverse osmosis membranes. *J. Membr. Sci.* **294**, 1–7.

Jiang, H. J., Moon, K. S., Zhang, Z. Q., Pothukuchi, S. & Wong, C. P. 2006 Variable frequency microwave synthesis of silver nanoparticles. *J. Nanopart. Res.* **8**, 117–124.

Kappachery, S., Paul, D., Yoon, J. & Kweon, J. H. 2010 Vanillin, a potential agent to prevent biofouling of reverse osmosis membrane. *Biofouling* **26**, 667–672.

Lee, H. S., Im, S. J., Kim, J. H., Kim, H. J., Kim, J. P. & Min, B. R. 2008 Polyamide thin-film nanofiltration membranes containing TiO_2 nanoparticles. *Desalination* **219**, 48–56.

Liao, C. J., Zhao, J. Q., Yu, P., Tong, H. & Luo, Y. B. 2010 Synthesis and characterization of SBA-15/poly (vinylidene fluoride) (PVDF) hybrid membrane. *Desalination* **260**, 147–152.

Lind, M. L., Ghosh, A. K., Jawor, A., Huang, X. F., Hou, W., Yang, Y. & Hoek, E. M. V. 2009 Influence of zeolite crystal size on zeolite-polyamide thin film nanocomposite membranes. *Langmuir* **25**, 10139–10145.

Liu, Y., Rosenfield, E., Hu, M. & Mi, B. 2013 Direct observation of bacterial deposition on and detachment from nanocomposite membranes embedded with silver nanoparticles. *Water Res.* **47**, 2949–2958.

Mafune, F., Kohno, J., Takeda, Y., Kondow, T. & Sawabe, H. 2000 Structure and stability of silver nanoparticles in aqueous solution produced by laser ablation. *J. Phys. Chem. B.* **104**, 8333–8337.

Majeed, S., Fierro, D., Buhr, K., Wind, J., Du, B., Boschetti-De-Fierro, A. & Abetz, V. 2012 Multi-walled carbon nanotubes (MWCNTs) mixed polyacrylonitrile (PAN) ultrafiltration membranes. *J. Membr. Sci.* **403**, 101–109.

Mollahosseini, A., Rahimpour, A., Jahamshahi, M., Peyravi, M. & Khavarpour, M. 2012 The effect of silver nanoparticle size on performance and antibacteriality of polysulfone ultrafiltration membrane. *Desalination* **306**, 41–50.

Qiu, S., Wu, L. G., Pan, X. J., Zhang, L., Chen, H. L. & Gao, C. J. 2009 Preparation and properties of functionalized carbon nanotube/PSF blend ultrafiltration membranes. *J. Membr. Sci.* **342**, 165–172.

Rana, D. & Matsuura, T. 2010 Surface modifications for antifouling membranes. *Chemical Reviews* **110**, 2448–2471.

Stankovich, S., Dikin, D. A., Piner, R. D., Kohlhaas, K. A., Kleinhammes, A., Jia, Y., Wu, Y., Nguyen, S. T. & Ruoff, R. S. 2007 Synthesis of graphene-based nanosheets via chemical reduction of exfoliated graphite oxide. *Carbon* **45**, 1558–1565.

Sun, M. P., Su, Y. L., Mu, C. X. & Jiang, Z. Y. 2010 Improved antifouling property of PES ultrafiltration membranes using additive of silica-PVP nanocomposite. *Ind. Eng. Chem. Res.* **49**, 790–796.

Taurozzi, J. S., Arul, H., Bosak, V. Z., Burban, A. F., Voice, T. C., Bruening, M. L. & Tarabara, V. V. 2008 Effect of filler incorporation route on the properties of polysulfone-silver nanocomposite membranes of different porosities. *J. Membr. Sci.* **325**, 58–68.

Tenover, F. C. 2006 Mechanisms of antimicrobial resistance in bacteria. *American J. Infect. Control.* **34**, S3–S10.

Wang, X. F., Chen, X. M., Yoon, K., Fang, D. F., Hsiao, B. S. & Chu, B. 2005 High flux filtration medium based on nanofibrous substrate with hydrophilic nanocomposite coating. *Environ. Sci. Technol.* **39**, 7684–7691.

Weng, T. H., Tseng, H. H. & Wey, M. Y. 2011 Effect of SBA-15 texture on the gas separation characteristics of SBA-15/polymer multilayer mixed matrix membrane. *J. Membr. Sci.* **369**, 550–559.

Wu, H., Tang, B. & Wu, P. 2010 Novel ultrafiltration membranes prepared from a multi-walled carbon nanotubes/polymer composite. *J. Membr. Sci.* **362**, 374–383.

Wu, H., Tang, B. & Wu, P. 2012 Novel hollow mesoporous silica spheres/polymer hybrid membrane for ultrafiltration. *J. Phys. Chem. C.* **116**, 2246–2252.

Wu, H., Tang, B. & Wu, P. 2013a Optimization, characterization and nanofiltration properties test of MWNTs/polyester thin film nanocomposite membrane. *J. Membr. Sci.* **428**, 425–433.

Wu, H., Tang, B. & Wu, P. 2013b Optimizing polyamide thin film composite membrane covalently bonded with modified mesoporous silica nanoparticles. *J. Membr. Sci.* **428**, 341–348.

Yin, J., Yang, Y., Hu, Z. & Deng, B. L. 2013 Attachment of silver nanoparticles (AgNPs) onto thin-film composite (TFC) membranes through covalent bonding to reduce membrane biofouling. *J. Membr. Sci.* **441**, 73–82.

Yu, H., Zhang, Y., Zhang, J., Zhang, H. & Liu, J. 2013 Preparation and antibacterial property of SiO_2-Ag/PES hybrid ultrafiltration membranes. *Desalin. Water Treat.* **51**, 3584–3590.

Zhang, M. Y., Zhang, K. S., De Gusseme, B. & Verstraete, W. 2012 Biogenic silver nanoparticles (bio-Ag-0) decrease biofouling of bio-Ag-0/PES nanocomposite membranes. *Water Res.* **46**, 2077–2087.

Zhang, X., Shi, B. & Liu, Y. 2013 Preparation of polysulfone ultrafiltration membranes modified by silver particles. *Desalin. Water Treat.* **51**, 3762–3767.

Zodrow, K., Brunet, L., Mahendra, S., Li, D., Zhang, A., Li, Q. L. & Alvarez, P. J. J. 2009 Polysulfone ultrafiltration membranes impregnated with silver nanoparticles show improved biofouling resistance and virus removal. *Water Res.* **43**, 715–723.

First received 13 September 2016; accepted in revised form 17 December 2016. Available online 2 February 2017